SEARCH FOR NEUTRINOLESS DOUBLE BETA DECAY IN ^{150}Nd WITH THE NEMO3 EXPERIMENT

GWENAELLE BROUDIN-BAY ON BEHALF OF THE NEMO COLLABORATION
Laboratoire de l'Accélérateur Linéaire,
Université Paris-Sud 11, CNRS/IN2P3, Bâtiment 200,
91898 Orsay cedex, France

The double beta decay experiment NEMO3 has been taking data since February 2003. The aim of the experiment is to search for neutrinoless double beta decay with 10 kg of enriched isotopes. Using 939 days of data, a preliminary result was obtained for ^{150}Nd: $T^{2\nu}_{1/2} = (9.20^{+0.25}_{-0.22}(stat.) \pm 0.62(syst.)) \times 10^{18}$ y. No neutrinoless double beta decay signal was observed and a limit on the half-life of the process was set to $T^{0\nu}_{1/2} > 1.8 \times 10^{22}$ y at 90% confidence level. An overview of the results previously obtained for other isotopes is also given.

1 Introduction

Neutrinoless double beta decay ($0\nu\beta\beta$) for a nucleus of atomic number A and charge Z is the process: $(A, Z) \rightarrow (A, Z+2) + 2e^-$. The process belongs to physics beyond the Standard Model as it violates the conservation of the total lepton number. Its observation would prove that the neutrino is a Majorana particle. Neutrinoless double beta decay may occur through several mechanisms, among which the decay with light neutrino exchange that would grant access to the mass scale. The half-life of the $0\nu\beta\beta$ process is then given by:

$$(T^{0\nu}_{1/2})^{-1} = |M^{0\nu}(A,Z)|^2 G^{0\nu}(Q,Z) \langle m_\nu \rangle^2 \tag{1}$$

with $M^{0\nu}(A, Z)$ a nuclear matrix element (NME) obtained from theoretical calculations, $G^{0\nu}(Q, Z)$ a phase space factor depending on the Q value of the process, and $\langle m_\nu \rangle$ the effective mass of the neutrino. This effective mass is given by $\langle m_\nu \rangle = \sum_{i=1}^{3} U^2_{ei} m_i$ where U_{ei} stands for the squared elements of the PMNS matrix and m_i the mass associated to the mass eigenstate i.

2 The NEMO3 experiment

2.1 The NEMO3 detector

The NEMO3 experiment has been taking data since February 2003. The detector is located in the Modane Underground Laboratory (LSM) under a rock cover of 4800 m water equivalent. It accommodates 10 kg of double beta emitter foils. With its cylindrical geometry, the NEMO3 detector is divided into 20 sectors in the middle of which the foils were installed. The main isotopes used for the search of the neutrinoless double beta decay are ^{100}Mo (∼7 kg) and ^{82}Se (∼1 kg). Smaller amount of other isotopes are also used to study the two-neutrino double beta

Table 1: Isotopes in the NEMO3 detector.

	^{100}Mo	^{82}Se	^{116}Cd	^{150}Nd	^{96}Zr	^{48}Ca	^{130}Te	^{nat}Te	Cu
Mass (g)	6914	932	405	36.6	9.4	7.0	454	491	621
$Q_{\beta\beta}(keV)$	3034	2995	2805	3367	3350	4772	2529		

decay ($2\nu\beta\beta$) process. The sectors containing the natural tellurium and the copper foils are dedicated to the background measurement. The mass of each isotope within the detector is summarized in Table 1.

The principle of the NEMO3 detector is the identification of the electrons in a double beta decay process and the measurement of their individual energy. Therefore, a tracking chamber is associated to a calorimeter. The tracking volume consists of 6180 drift cells operated in Geiger mode. It allows the reconstruction of the trajectory of charged particles and the determination of the position of the vertex with a resolution of 5 mm tranversely to the source foil plane and 8 mm longitudinally. A 25 Gauss magnetic field is generated by a coil surrounding the detector and allows the identification of the charge of the particles. The drift gas inside the tracking volume is helium with added ethyl alcohol (4%), argon (1%) and water (0.1%). The calorimeter consists of 1940 photomultiplier tubes associated to plastic scintillator blocks. The energy resolution ranges from 14.1% to 17.7% for 1 MeV electrons. The time resolution is 250 ps. The tracker - calorimeter association allows to identify electrons, positrons, gammas and alpha particles as well as to measure their time of flight. The detector is protected from gammas by an iron shielding, and from neutrons present inside the laboratory by wood and a borated water shielding. A tent coupled to a radon-free air factory surrounds the detector. A detailed description of the detector was published in [1].

2.2 Background model

The background sources can be classified into three groups: the external background from incoming γ, the radon present inside the tracker volume and the internal background from radioactive contamination of the sources. The activities of theses background sources can be obtained through the use of a set of control channels corresponding to different event topologies on the NEMO3 data. These measured activities were compared to measurements performed with HPGe and radon detectors.

At the beginning of the experiment, the radon inside the tracking chamber, and more precisely the decay product ^{214}Bi present in its radioactive chain, was found to be the predominant background source. Radon is present in the air of the laboratory as it originates from the rock surrounding it and can penetrate inside the detector through small leaks. A tent coupled to radon-free air factory was then installed around the detector in October 2004 in order to decrease the presence of radon inside the tracker. The data taken before that date are referred to as Phase I data. After October 2004, the data are Phase II data.

3 NEMO3 results

3.1 $2\nu\beta\beta$ decay of ^{150}Nd

Measurements of the $2\nu\beta\beta$ half-life can be performed for 7 isotopes in the NEMO3 experiment. This process is the following: $(A,Z) \rightarrow (A,Z+2) + 2e^- + 2\bar{\nu}_e$. It constitutes the ultimate background in the $0\nu\beta\beta$ search because of the energy resolution of the detector.

The $\beta\beta$ type events are selected by requiring two tracks with a curvature compatible with a negative charge. Each track is associated to a separate energy deposit in the calorimeter greater than 200 keV. Both track should originate from a common vertex located inside the source foil. The time of flight measurement for both electrons must be consistent with the hypothesis that they were emitted from the foil.

A preliminary measurement of the half-life of ^{150}Nd was obtained for a 36.6 g sample from data collected between February 2003 and December 2006, corresponding to 939 days of data taken during the Phases I and II of the experiment. A total of 2828 $\beta\beta$ type events were observed with a signal-over-background ratio of 2.7. The distribution of the energy sum of the electrons in $\beta\beta$ type events and the angle between them are shown in Fig. 1. The background substracted data and the $2\nu\beta\beta$ signal expectation obtained from Monte-Carlo are in good agreement. The $2\nu\beta\beta$ selection efficiency is 7.2%. The measured half-life is $T_{1/2}^{2\nu} = (9.20^{+0.25}_{-0.22}(stat.) \pm 0.62(syst.)) \times 10^{18}y$. This value is in between two previous results obtained from experiments led using time projection chambers [2], [3].

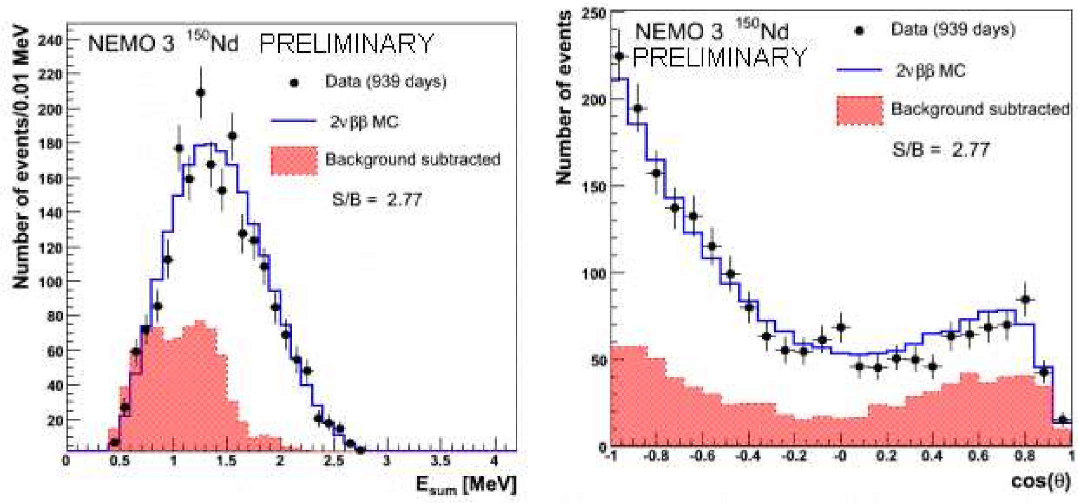

Figure 1: Distribution of the energy sum of the two electrons E_{sum} (left graph) and the angle between the two electrons $cos\theta$ (right graph), background substracted. The data are shown as points and the substracted background as a red histogram.

3.2 $2\nu\beta\beta$ decay of other isotopes

The half-life of the $2\nu\beta\beta$ process for the other isotopes inside NEMO3 was measured using the data from Phase I or combined Phases I and II and the preliminary results are given in Table 2. These results are important for nuclear theory as they help constrain the nuclear models and thus improve the NME calculations. The NME are a source of uncertainty when translating the half-lives of the $0\nu\beta\beta$ into effective neutrino masses.

3.3 Search for neutrinoless double beta decay of ^{150}Nd

A $0\nu\beta\beta$ decay signal would correspond to an excess of $\beta\beta$ type events around the energy of the transition $Q_{\beta\beta}$ in the distribution of the energy sum of the electrons. Indeed, the theoretical peak at $Q_{\beta\beta}$ would be smeared out by the energy resolution of the calorimeter. For ^{150}Nd, the $Q_{\beta\beta}$ value is 3.367 MeV. Fig. 2 shows that no excess of events in the distribution of the energy sum of the electrons for the $\beta\beta$ type events originating from the ^{150}Nd sample is observed for 939 days of data collection. A limit on the half-life of the $0\nu\beta\beta$ process was subsenquently set using the CL_s method [5] for $E_{sum} > 2.5$ MeV. The corresponding $0\nu\beta\beta$ selection efficiency is 19%. The limit on the half-life obtained is $T_{1/2}^{0\nu} > 1.8 \times 10^{22}$ years at 90% confidence level (CL), which translates into an upper limit on the effective Majorana mass of the neutrino in the range

Table 2: Half-lives of $2\nu\beta\beta$ processes measured using Phase I data (360 days). The ^{130}Te results use Phases I and II data (534 days).

Isotope	Signal/Background	$T_{1/2}$ [10^{19} years]
^{100}Mo	40	$0.711 \pm 0.002(stat.) \pm 0.054(syst.)$ [4]
^{82}Se	4	$9.6 \pm 0.3(stat.) \pm 1.0(syst.)$ [4]
^{116}Cd	7.5	$2.8 \pm 0.1(stat.) \pm 0.3(syst.)$
^{96}Zr	1	$2.0 \pm 0.3(stat.) \pm 0.2(syst.)$
^{48}Ca	~ 10	$3.9 \pm 0.7(stat.) \pm 0.6(syst.)$
^{130}Te	0.25	$76 \pm 15(stat.) \pm 8(syst.)$

$\langle m_\nu \rangle < 1.9 - 2.7$ eV according to the NME calculations in[7] and $\langle m_\nu \rangle < 5.4 - 8.5$ eV according to [8]. The limit on the half-life was improved by one order of magnitude compared to the previous result, $T^{0\nu}_{1/2} > 1.7 \times 10^{21}$ years at 90% CL [6].

Along with the light neutrino exchange, other mechanisms can mediate $0\nu\beta\beta$ decay. Among those can be found the models with Majoron emission characterized by a spectral index n and the model with a right-handed (V+A) contribution in the Lagrangian. In the assumption of a $0\nu\beta\beta$ process involving right currents (V+A), the limit on the half-life was found to be $T^{0\nu}_{1/2} > 1.27 \times 10^{22}$ years at 90% confidence level. For a $0\nu\beta\beta$ process with the emission of a Majoron (spectral index $n = 1$) the limit obtained is $T^{0\nu}_{1/2} > 1.55 \times 10^{21}$years at 95% CL.

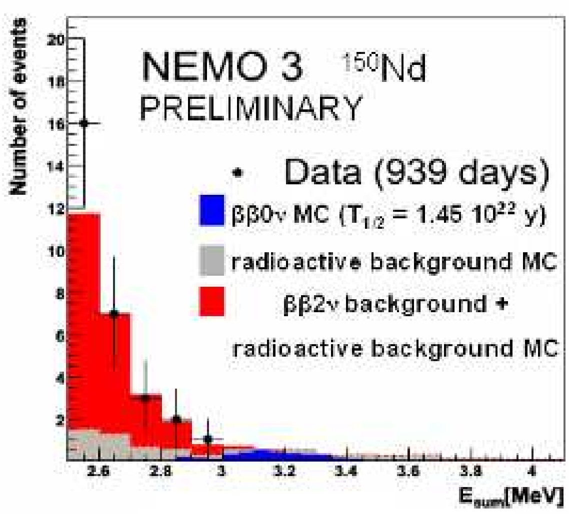

Figure 2: Distribution of the energy sum of the two electrons E_{sum} for $E_{sum} > 2.5$ MeV for data (points) compared to the total background (in red) consisting of the radioactive background (in grey) plus the $2\nu\beta\beta$. A MC simulation of a $0\nu\beta\beta$ signal with a half-life of 1.45×10^{22} years is shown in blue.

3.4 Search for $0\nu\beta\beta$ of ^{100}Mo and ^{82}Se

^{100}Mo and ^{82}Se are the main isotopes in the NEMO3 detector used for the search for neutrinoless double beta decay. For both isotopes, 639 days of data spread over the two phases of the experiment were analyzed. For ^{100}Mo the $Q_{\beta\beta}$ value is 3.034 MeV. No excess of events was found in the $2.8 < E_{sum} < 3.2$ MeV energy window, as 12.1 events are expected from Monte Carlo and 11 were observed. The $0\nu\beta\beta$ selection efficiency is 8.2%, which leads to a limit on the

Table 3: Constraints on $T_{1/2}$ in years (90% CL) for (V+A) and Majoron emission processes from NEMO3 data. λ is a (V+A) Lagrangian parameter and g is a Majoron to neutrino coupling strength.

$0\nu\beta\beta$ process	^{100}Mo	^{82}Se
(V+A) current	$> 3.2 \times 10^{23}$ $\lambda < 1.8 \times 10^{-6}$	$> 1.2 \times 10^{23}$ $\lambda < 2.8 \times 10^{-6}$
$n = 1$	$> 2.7 \times 10^{22}$ $g <$ (0.4 - 1.8) $\times 10^{-4}$	$> 1.5 \times 10^{22}$ $g <$ (0.7 - 1.9) $\times 10^{-4}$
$n = 3$	$> 1.7 \times 10^{22}$	$> 6.0 \times 10^{21}$
$n = 5$	$> 1.0 \times 10^{22}$	$> 3.1 \times 10^{21}$
$n = 7$	$> 7.0 \times 10^{19}$	$> 5.0 \times 10^{20}$

half-life of the $0\nu\beta\beta$ process $T^{0\nu}_{1/2} > 5.8 \times 10^{23}$ years at 90% CL. This translates into an upper limit on the neutrino mass of $\langle m_\nu \rangle < 0.8 - 1.3$ eV using the values of the NME in [9]. The $Q_{\beta\beta}$ value for ^{82}Se is 2.995 MeV. As for ^{100}Mo, no excess of events was found around the $Q_{\beta\beta}$ value in the distribution of the energy sum of the electrons. In the $2.65 < E_{sum} < 3.20$ MeV energy window, 7 events were observed for 6.4 estimated by Monte Carlo simulations. With a 14.4% $0\nu\beta\beta$ selection efficiency, the obtained limit on the half-life is $T^{0\nu}_{1/2} > 2.1 \times 10^{23}$ years at 90% CL. The corresponding upper limit on the mass of the neutrino using [10] is then $\langle m_\nu \rangle < 1.4 -$ 2.2 eV. The results obtained for the half-life of the $0\nu\beta\beta$ process of ^{100}Mo and ^{82}Se through the (V+A) and the Majoron mechanisms [11] are summarized in Table 3.

4 Summary

The NEMO3 experiment allows the measurement of $2\nu\beta\beta$ decays with very high statistics. A preliminary result was obtained for the $2\nu\beta\beta$ half-life of ^{150}Nd for a 36.6 g sample: $T^{2\nu}_{1/2} = (9.20^{+0.25}_{-0.22}(stat.) \pm 0.62(syst.)) \times 10^{18}$ years. A limit on the the $0\nu\beta\beta$ half-life of $T^{0\nu}_{1/2} > 1.8 \times 10^{22}$ years was estimated at 90 % confidence level. The $Q_{\beta\beta}$ value of ^{150}Nd is one of the highest among $\beta\beta$ emitters and lies above the typical energies of many background sources. Also, that isotope has a large phase space factor. These characteristics make ^{150}Nd a promising candidate for the SuperNEMO experiment aiming at a sensivity of 50 meV on the Majorana neutrino mass with 100 kg of enriched isotopes. The enrichment process is currently under study by the Nd-150 collaboration for the SuperNEMO and SNO++ projects.

References

1. R. Arnold et al., Nucl. Instr. Meth. A 536 (2005) 79.
2. V. Artemiev et al., Phys. Let. B, 345, (1995), 564.
3. A. De Silva et al., Phys. Rev. C 56 (1997) 2451.
4. R. Arnold et al., Phys. Rev. Lett. 95 182302 (2005).
5. W. Fisher, FERMILAB-TM 2386-E (2007).
6. A. A. Klimenko et al., Nucl. Instr. Meth. B17 (1986) 445.
7. V. A. Rodin et al., Nucl. Phys. A 793 (2007) 231.
8. J. G. Hirsch et al., Nucl. Phys. A 582 (1995) 124.
9. V. A. Rodin et al., Nucl. Phys. A 793, (2007) 213; F. Simkovic et al., Phys. Rev. C 60, 055502 (1999) ; M. Aunola et al., Nucl. Phys. A 643, 207 (1998) ; J. Suhonen et al., Nucl. Phys. A 273, 271 (2003) ; S. Stoica et al., Nucl. Phys. A 694, 269 (2001).
10. V. A. Rodin et al., Nucl. Phys. A 793, (2007) 213; M. Kortelainen and J. Suhonen, Phys.

Rev. C 75, (2007) 051303(R); M. Kortelainen and J. Suhonen, Phys. Rev. C 75, (2007) 024315.
11. R. Arnold et al., Nucl. Phys. A 765 (2006) 483.